Fluorescence Excitation Spectroscopy of the 3p Rydberg States of 1-Azabicyclo[2.2.2]octane and 1-Azaadamantane

Jurriaan M. Zwier and Albert M. Brouwer*

Institute of Molecular Chemistry, Laboratory of Organic Chemistry, University of Amsterdam, Nieuwe Achtergracht 129, 1018 WS Amsterdam, The Netherlands

Arjan Rijkenberg and Wybren Jan Buma*

Institute of Molecular Chemistry, Laboratory for Physical Chemistry, University of Amsterdam, Nieuwe Achtergracht 127-129, 1018 WS Amsterdam, The Netherlands

Received: June 17, 1999; In Final Form: October 18, 1999

The singlet states of the 3p Rydberg manifold of the structurally rigid amines 1-azabicyclo[2.2.2]octane and 1-azaadamantane seeded in supersonic expansions have been investigated by means of fluorescence excitation spectroscopy. Under these conditions a better spectral resolution could be obtained than in previous studies, enabling us to resolve and identify unambiguously the 0_0^0 transitions to the second and third excited singlet states. These states are assigned as the 1^1E and 3^1A_1 states, associated with excitation of a lone-pair electron to the $3p_{x,y}$ and $3p_z$ Rydberg orbitals, respectively. Analysis of the vibrational energies and intensities of vibronic transitions observed in the excitation spectra of both states leads to the conclusion that the equilibrium geometry and vibrational properties of the molecule in these two states resemble closely those of the lowest excited singlet state, which derives from excitation of a lone-pair electron to the 3s Rydberg orbital, and those of their ionic core. Excitation spectra in combination with dispersed emission spectra and fluorescence decays demonstrate that internal conversion to the lowest excited singlet state shows up prominently in the dynamics of the 3p Rydberg states.

Introduction

Saturated amines such as 1-aza[2.2.2]bicyclooctane (ABCO) and 1-azaadamantane (AADA) (Figure 1) have a particular appeal to spectroscopists and synthetic chemists alike as a result of their rigid cagelike structure. They are employed, for example, as donor moieties in intramolecular electron-donor−acceptor systems[1−5] and form part of natural products such as quinine. From a spectroscopic point of view they are of considerable interest as the cagelike structure inhibits large structural changes in the geometry around the nitrogen atom upon excitation. It is by now well established that the electronically excited states of these compounds and saturated amines in general can ultimately be related to the excited states of ammonia, the most simple representative of this class of compounds; i.e., the lower excited states derive from the excitation of a lone-pair electron to Rydberg orbitals.[6] Excitation spectra of saturated alkylamines are usually diffuse and vibrational structure is not observable. "Locking" of the molecular geometry in structurally rigid amines in general—and ABCO and AADA in particular—leads, however, to vibrationally well-resolved excitation spectra, which can be fruitfully employed to investigate the geometric and electronic structure of excited states, as well as their dynamic properties.

Recently we have investigated the lowest excited singlet states of ABCO and AADA using fluorescence excitation and dispersed emission spectroscopy, ultimately aiming to determine mode-specific reorganization energies accompanying ionization of the molecule, one of the key factors in rate expressions for electron transfer in intramolecular electron-donor−acceptor systems.[7] The application of supersonic expansion techniques

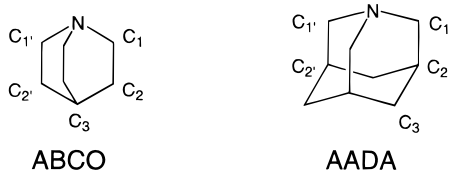

Figure 1. Structures and atom numbering of 1-azabicyclo[2.2.2]octane (ABCO) and 1-azaadamantane (AADA).

enabled us to obtain high-quality excitation and emission spectra, which exhibited a plethora of vibronic transitions. It was shown that a very detailed analysis of these spectra was possible on the basis of the concept that the geometric and vibrational properties of the lowest excited singlet state of these compounds—the $[X\ ^2A_1]3s$ Rydberg state—are expected to resemble to a large extent those of its ionic core. Accordingly, the equilibrium geometry and force field of the ground state of the neutral molecule and its radical cation were determined by density functional theory (DFT) calculations and subsequently employed to predict the experimentally obtained excitation spectra. The quantitative agreement between experimental and predicted spectra that was achieved after correcting for some minor geometrical differences between the equilibrium geometries of the lowest excited singlet state and the ground state of the radical cation confirmed our initial working hypothesis and allowed us to extract valuable information on the properties of these states, such as mode-specific reorganization energies and the role of vibronic coupling.

In the present study we will be concerned with the higher-lying second and third excited singlet states of the two compounds. These states derive in a zeroth-order Rydberg

10.1021/jp992001n CCC: $19.00
Published on Web 01/07/2000

picture from the excitation of a lone-pair electron to the 3p Rydberg orbital. In the molecular symmetry point group of the molecules (C_{3v}) the 3p Rydberg state is split into the 1^1E and 3^1A_1 states, associated with excitation to the $3p_{x,y}$ and $3p_z$ components, respectively. In polyatomic species of the size of the present ones the core splitting between the various components of an—in spherical symmetry degenerate—Rydberg state is in general difficult to resolve due to the congestion of vibronic bands in absorption and excitation spectra. Indeed, the stronger vibronic transitions present in the room-temperature excitation spectrum of the 3p Rydberg state of ABCO could only be assigned to the 1^1E or 3^1A_1 state by comparison of their intensities in one- and two-photon excitation and by their polarization behavior under two-photon excitation conditions.[8] Detailed studies under high-resolution conditions have, however, not been reported yet. The 3p Rydberg states of AADA are in this respect even more poorly studied: only absorption spectra at room temperature have been obtained of which the vibronic structure has generically been assigned to the 3p Rydberg state.[2,9,10] Here we will show that the spectroscopic and dynamic properties of the 3p Rydberg states of ABCO and AADA can successfully be studied by the same techniques employed for the study of the lowest excited singlet state.

Experimental Details

The present experiments have been performed analogously to our previously reported experiments on the lowest excited singlet state of the two title compounds.[7] Briefly, fluorescence excitation and dispersed emission spectroscopy was applied on samples seeded in a continuous supersonic jet, created by expanding 3 bar He through a nozzle with an aperture of 0.1 mm. Excitation with laser light from a frequency-doubled dye laser operating either on Coumarine 480, Coumarine 460, or Coumarine 440 and pumped by a XeCl excimer laser working at a repetition rate of 60 Hz occurred at 10 nozzle diameters, i.e., 1.0 mm, from the nozzle. Fluorescence from the jet-cooled compounds was collected at right angles with respect to the excitation light and the molecular beam, dispersed in a monochromator employed in second order, and detected with a photomultiplier.

For recording excitation spectra, the monochromator was used with a slit width of 5 mm, resulting in a spectral resolution of 25 nm in second order. In the investigated excitation energy regions it was found that maximum emission could be collected when center emission wavelengths of 543 (271.5 in second order) and 575 (287.5) nm for ABCO and AADA, respectively, were used, i.e., wavelengths for which previously the maximum of emission was found when exciting the lowest excited singlet state. In a typical experiment, excitation spectra were obtained by scanning the dye laser in steps of 1.0 cm^{-1} in the case of ABCO and 0.5 cm^{-1} in the case of AADA, averaging over 10 laser pulses, and dividing the signal by the laser intensity.

ABCO was obtained from Aldrich and was used without further purification. AADA was synthesized by Wolff—Kishner reduction of 1-azaadamantanone.[11]

Results and Discussion

1-Azabicyclo[2.2.2]octane. Figure 2 displays the one-photon fluorescence excitation spectrum of ABCO in the energy region from 43 200 to 46 200 cm^{-1}. Previous experiments on samples at room temperature,[8,12−14] and in particular the comparison of one- and two-photon excitation spectra,[8] led to the conclusion that vibronic transitions to the $S_2(1^1E)$ and $S_3(3^1A_1)$ states, which have been associated with the $3p_{x,y}$ and $3p_z$ Rydberg states,

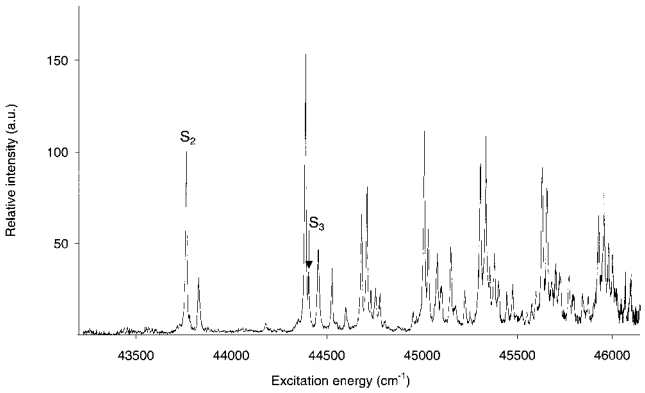

Figure 2. Fluorescence excitation spectrum of the 1^1E (S_2) ← S_0 and 3^1A_1 (S_3) ← S_0 transitions of 1-azabicyclo[2.2.2]octane. The 0_0^0 transitions are found at 43 763 and 44 404 cm^{-1}.

respectively, are located in this energy region. The general appearance of the spectrum is in good agreement with previously obtained results, but due to vibrational and rotational cooling of the molecule in the supersonic expansion the present spectrum exhibits considerable narrowing of the resonances. As a result, considerably more vibronic transitions can be observed. Guided by our analysis of the $S_1 \leftarrow S_0$ excitation spectrum, the analysis of the spectrum shown in Figure 2 leads indeed to the conclusion that it consists of a superposition of two excitation spectra built upon 0_0^0 transitions located at 43 763 and 44 404 cm^{-1}, respectively. These energies differ slightly from previously reported values of 43 750 and 44 390 cm^{-1},[8] which might be attributed to the difference in resonance widths in the two experiments; in the present experiments a width of about 9 cm^{-1} is obtained, while reported spectra at room temperature indicate a width of at least 60 cm^{-1}. Our experiments show that the intensities of the two 0_0^0 transitions are in the ratio of 3:1 (S_2:S_3). It is interesting to notice that this ratio is in excellent agreement with the oscillator strength calculations of Avouris and Rossi.[15] These have been performed at a level of ab initio theory which would nowadays be considered as rather low, but ironically, calculations performed subsequently at a higher level of theory fail to reproduce this ratio.[16]

The frequencies and intensities of identified $(\nu_i)_0^1$ transitions to the S_2 and S_3 states are reported in Table 1. In agreement with our a priori expectations, the frequencies and intensities of vibronic transitions involving totally symmetric vibrations are quite similar to what is observed in the excitation spectrum of the lowest excited singlet state: the spectrum is dominated by the cage-squashing mode ν_{12} and exhibits considerable activity in the ν_{11} (bending of $C_1NC_{1'}$ and $C_1C_2C_3$), ν_9 (C_1C_2 stretch), and ν_8 (cage deformation) modes. These activities are by now well understood as reflecting the geometrical response of the molecule to the excitation of a lone pair electron to a nonbonding Rydberg orbital and the corresponding change from a purely sp^3-hybridized to a more sp^2-like nitrogen atom. The similarity observed between the excitation spectra of the various Rydberg states implicitly supports our assumption that the equilibrium geometry and vibrational properties of these Rydberg states are predominantly determined by their ionic core; i.e., the Rydberg electron does not exert a significant influence on these properties. Indeed, Table 1 shows that the observed vibrational frequencies and transition intensities match impressively well those predicted on the basis of the equilibrium geometry and force field of the ground state of the radical cation.

Apart from the activity of totally symmetric vibrations, the $S_1 \leftarrow S_0$ excitation spectrum also shows transitions to nontotally

TABLE 1: Experimental Vibrational Frequencies (cm^{-1}) and Intensities of $(\nu_i)_0^1$ Transitions in the Fluorescence-Detected Excitation Spectra of Excited Singlet States of ABCO

		$S_2(1\ ^1E)^a$		$S_3(3\ ^1A_1)^a$		$S_1(2\ ^1A_1)^b$		$D_0(1\ ^2A_1)^c$	
mode		freq	int[d]	freq	int[d]	freq	int[d]	freq	int[d]
a_1	ν_{12}	623	157	627	166	626.1	97	637.4	111
	ν_{11}	764	37	772	46	774.3	63	782.2	30
	ν_{10}	786	7			789.0	5	790.0	3
	ν_9	919	66	926[e]		922.0	61	932.0	75
	ν_8	947	85	951	100	937.3	54	947.8	62
	ν_7	1287	10			1263.2	39	1320.2	38
	ν_6	1337	23			1332.3	9	1377.0	9
	ν_5					1463.7	5	1519.8	0
	ν_4					1541.3	2	1560.1	3
e	ν_{37}	418	7	417	11	413.3	1	420.8	
	ν_{34}			847	37	859.4	2	853.9	
	ν_{33}	968	25			985.9	1	987.8	

[a] Present work. [b] Results obtained in fluorescence excitation studies of the $S_1 \leftarrow S_0$ transition.[7] [c] Frequencies and intensities predicted from (U)B3LYP/6-311G* calculations on equilibrium geometry and harmonic force field of the ground state of the neutral molecule and its radical cation.[7] [d] Intensities taken with respect to intensity of 0_0^0 transition, which is taken as 100. [e] The 9_0^1 transition to S_3 cannot be observed directly since it overlaps with the strong $12_0^1 8_0^1$ transition to S_2. Instead, the frequency of ν_9 has been deduced from the $12_0^1 9_0^1$ transition to S_3.

symmetric vibrational levels of e symmetry, which was taken as evidence for an important role of vibronic coupling between the first and second excited singlet state.[7] The widths of the resonances in the present work do not allow as many vibrations of e symmetry to be identified as in our previous study on the lowest excited singlet state S_1, but an unambiguous sign that vibronic coupling also plays a role in the spectroscopy of S_2 and S_3 can be found in the isolated resonances 418 and 417 cm^{-1} above the 0_0^0 transitions to the S_2 and S_3 states, respectively, which can only be assigned to 37 $(e)_0^1$ transitions.

The excitation spectra reported earlier by Weber et al.[8] and by Halpern et al.[11] exhibited a shoulder on the high-energy side of the 0_0^0 transition to the S_2 state, which the authors did not comment upon. The higher spectral resolution attained in the present excitation spectrum enables us to observe this shoulder as an isolated resonance at 65 cm^{-1} above the 0_0^0 transition and its combination bands with the dominant resonances involving single or combinations of totally symmetric vibrations. Calculated and observed frequencies of a_1 and e vibrations in the S_0, S_1, and D_0 states exclude an assignment to excitation of such vibrational modes and indicate that this band involves excitation of a vibrational level of the lowest-frequency a_2 torsional mode ν_{19} with one or two quanta.[7] Spectral congestion in combination with the widths of the resonances and the lower intensity of the 0_0^0 transition to S_3 preclude the identification of any low-frequency band that might be associated with a similar transition to this state.

To come to an assignment of the 65 cm^{-1} band, we consider first what is known of the vibrational levels of ν_{19} in other neutral and ionic states. Studies of the $S_1 \leftarrow S_0$ excitation spectrum of ABCO have revealed that this mode is highly (positive) anharmonic in the ground and excited states.[17] Due to the conservation of C_{3v} symmetry of the molecule upon excitation, the dominant band in the excitation spectrum of S_1 involving this mode derives from the 19_0^2 transition, found 134 cm^{-1} above the 0_0^0 transition.[7,17,18] Since in the ground state of the neutral molecule and its radical cation the $\nu_{19}(v = 2)$ level is located at 87 [17] and 77 cm^{-1},[18] respectively, it has been concluded that the cage is more rigid in S_1 than in S_0 and D_0.[17]

Assuming that the molecule retains C_{3v} symmetry upon excitation to S_2, the 65 cm^{-1} band per se needs to be assigned to the 19_0^2 transition. In that case one would conclude that the potential energy surface of S_2 along the ν_{19} normal coordinate resembles that of D_0—as might be expected on the basis of a description of S_2 as a Rydberg state consisting of an ionic core D_0 with a nonbonding Rydberg electron—and that the rigidity of the cage is similar in S_0, S_2, and D_0. Although we prefer indeed this assignment over its alternative (vide infra), the intensity of the 65 cm^{-1} band (31% of the intensity of the 0_0^0 transition) seems rather high in view of the intensity of the same transition in the $S_1 \leftarrow S_0$ excitation spectrum (6% of the intensity of the 0_0^0 transition) and the absence of additional members of a 19_0^n progression. While the intensity of the 19_0^2 ($S_1 \leftarrow S_0$) transition can be rationalized reasonably well on account of the almost 2-fold increase in frequency upon excitation and the anharmonicity of the vibration, an increase of the intensity of the same transition to S_2 would seem to be at odds with the similarity of the potential energy surfaces of S_0 and S_2 along ν_{19}. The high intensity of this transition might therefore be taken as evidence that the Condon approximation is not valid for this transition, i.e., that the $S_2 \leftarrow S_0$ electronic transition moment changes significantly as a function of the ν_{19} normal coordinate.

As an alternative, an assignment to the 19_0^1 transition might be considered. This assignment would imply that excitation to S_2 is accompanied by a reduction of the molecular symmetry from C_{3v} to at most C_3. Calculation of the displacement needed in the harmonic approximation to account for the observed intensity indicates that one deals with relatively small geometrical changes (5° in the $NC_1C_2C_3$ dihedral angle), but the nondegeneracy of ν_{19} implies at the same time that the potential energy surface of S_2 along this coordinate is a double-minimum potential with minima of equal energy. Combined with the low frequency of ν_{19} and the small—calculated—displacement from the C_{3v} geometry, significant tunneling effects can be expected. Observation of the 19_0^1 transition therefore leads one to expect that also 19_0^n ($n > 1$) transitions should have an observable intensity, at odds with our experimental observations. We consequently tend to favor the previously suggested 19_0^2 assignment.

When the intensities of $(\nu_i(a_1))_0^1$ transitions are considered in more detail, we see that some differences are present between the $S_1 \leftarrow S_0$ and $S_2 \leftarrow S_0$ excitation spectra, in particular with respect to the activity of ν_{12}. This indicates that the equilibrium geometry of the molecule in S_1 is slightly different from the one in S_2. To get an idea of what kind of geometry differences we are dealing with, we have applied the same procedure as employed previously in the reconstruction of the geometry of the lowest excited singlet state;[7] i.e., we assume that the calculated equilibrium geometry of S_0 as well as the calculated normal coordinates of S_0 and D_0 are "exact", take the normal coordinates of S_2 the same as those of D_0, and use the experimentally observed intensities of $(\nu_i(a_1))_0^1$ transitions to calculate the displacement vector. The resulting parameters given in Table 2 show that small changes in bond lengths and valence angles already account for the observed differences in transition intensities and that the equilibrium geometry of the molecule in both states closely resembles that of the ground-state D_0 of the radical cation. A similar analysis for the equilibrium geometry of S_3 is not warranted in view of the limited number of transitions to this state that can be identified. The observation

TABLE 2: Selected Geometrical Parameters (Å, deg) of the Equilibrium Geometry of the Ground State of ABCO (S_0) and Its Radical Cation (D_0) and of the First (S_1) and Second (S_2) Excited Singlet States

	$S_0(1\,^1A_1)^a$	$S_1(2\,^1A_1)^{b,e}$	$S_2(1\,^1E)^{c,e}$	$D_0(1\,^2A_1)^{d,e}$
$N-C_1$	1.472	−0.034	−0.023	−0.024
C_1-C_2	1.562	0.038	0.023	0.036
C_2-C_3	1.541	0.001	−0.003	−0.005
C_1-H_1	1.094	0.000	0.000	−0.005
C_2-H_2	1.095	0.000	0.000	−0.004
C_3-H_3	1.094	0.000	0.000	0.001
$C_1NC_{1'}$	109.3	5.3	5.6	5.3
NC_1H_1	107.8	1.7	0.8	1.7
NC_1C_2	111.8	−6.3	−7.2	−6.8
$C_1C_2H_2$	111.1	−2.4	−2.2	−2.3
$C_1C_2C_3$	108.0	0.1	0.5	0.1
$C_2C_3H_3$	110.2	−0.2	−0.4	−0.7
$C_2C_3C_{2'}$	108.7	0.2	0.4	0.7

[a] B3LYP/6-311G* optimized geometry.[7] [b] Previously reconstructed geometry from $S_1 \leftarrow S_0$ fluorescence excitation studies.[7] [c] Present work. [d] UB3LYP/6-311G* optimized geometry.[7] [e] Given as changes with respect to the geometry of S_0.

that for this state the 12_0^1, 11_0^1, and 8_0^1 transitions have similar intensities as for S_2 might be taken as qualitative evidence that its equilibrium geometry resembles more the one of the molecule in S_2 than in S_1.

Apart from elucidating their spectroscopic properties, the results of the present study also shed light on the dynamic properties of the 3p Rydberg states. Consider for example the line widths of the resonances in the excitation spectrum. In the beginning of this section we noticed that seeding of the sample in a supersonic jet expansion leads to considerable cooling of the vibrational and rotational degrees of freedom. Despite this cooling, the resonances retain a width of about 9 cm^{-1} for transitions to S_2 and S_3, which is significantly larger than the width of the resonances observed previously under the same conditions in the excitation spectrum of the lowest excited singlet state,[7] e.g., the 0_0^0 transition to S_1 shows a strong unresolved Q branch with a width of 0.3 cm^{-1} and weaker, partially rotationally resolved, P and R branches with a width of 1.5 cm^{-1}. We must consequently conclude that the resonances in the excitation spectra of S_2 and S_3 are lifetime broadened. Such a conclusion would seem to be at odds with a measurement of the fluorescence decay from both states, since upon excitation of the vibrationless level of S_1 the emission decays with a time constant of 260 ns, in agreement with a previously reported value,[9] while excitation of the vibrationless levels of both S_2 and S_3 leads to fluorescence with a decay time of 35 ns. The solution to the apparent contradiction between a resonance width of 9 cm^{-1} and decay times on a nanosecond time scale is found by considering the dispersed emission. As mentioned in the Experimental Section, the maximum of emission intensity has been found at a detection wavelength equal to that employed in the fluorescence excitation experiments on the lowest excited singlet state. Indeed, emission spectra obtained after excitation of various vibrational levels in either the second or third excited singlet state are broad and unresolved, significantly displaced from the frequency of the exciting light, and commence roughly at an energy consistent with the S_0-S_1 energy gap. The overall picture that therefore emerges is that excitation of S_2 or S_3 is followed by rapid internal conversion on a picosecond time scale to isoenergetic highly excited vibrational levels of S_1, which subsequently decay on a nanosecond time scale.

1-Azaadamantane. Figure 3 shows the one-photon fluorescence detected excitation spectrum of AADA in the energy region from 41 600 to 44 600 cm^{-1}, where transitions to the 3p Rydberg states are expected to occur. The use of a supersonic jet expansion leads here also to an increased spectral resolution, but as was also noticed in our previous study on the first excited singlet state,[7] vibrational cooling is less efficient than in the case of ABCO. As a result, a significant number of hot bands are visible in the spectrum. Although these hot bands complicate the assignment of the weaker features in the spectrum, its analysis leads straightforwardly to the conclusion that it is composed of the excitation spectra of two states, whose 0_0^0 transitions are located at 42 280 and 42 798 cm^{-1}. In analogy with the case of ABCO we assign the excitation spectrum of S_2 built upon the 42 280 cm^{-1} origin transition to the $3p_{x,y}$ 1^1E Rydberg state and the higher-lying S_3 state to the $3p_z$ 3^1A_1 state. Figure 3 demonstrates that the 3p Rydberg states are rather susceptible to, at first sight, small changes in the molecular structure: while in ABCO the two 0_0^0 transitions have an intensity ratio of 3:1 (S_2:S_3), a ratio of 14:1 is obtained for AADA. Moreover, the splitting between the two states is reduced from 641 cm^{-1} in ABCO to 518 cm^{-1} in AADA.

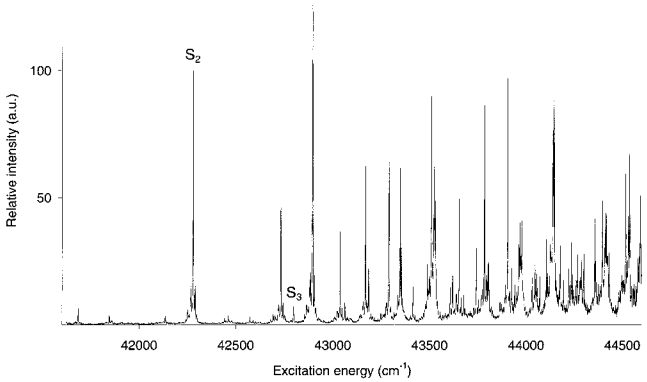

Figure 3. Fluorescence excitation spectrum of the 1^1E (S_2) ← S_0 and 3^1A_1 (S_3) ← S_0 transitions of 1-azaadamantane. The 0_0^0 transitions are found at 42 280 and 42 798 cm^{-1}.

The spectrum shown in Figure 3 enables for S_2 an accurate determination of the frequency of various totally symmetric vibrations and the intensity of the associated $(\nu_i)_0^1$ transition (Table 3). Despite the relatively small oscillator strength of the transition to S_3, the presence and identification of a significant number of overtone and combination bands allows us to determine with confidence the frequencies of such vibrations for this state (Table 3). The intensities of $(\nu_i)_0^1$ transitions to S_3 reported in Table 3 should, however, be considered more as qualitative than as quantitative, since (i) the intensity of the 0_0^0 transition is small, (ii) the $(\nu_i)_0^1$ transitions are located in energy regions where also hot bands to S_2 occur, and (iii) these transitions are located on the higher-energy side of the spectrum where, as Figure 3 shows, an increasing background signal is observed. The excitation spectrum of the lowest excited singlet state exhibited clear signs of vibronic coupling by the presence of transitions to nontotally symmetric vibrational levels. Unfortunately, the widths of the resonances in combination with the presence of hot bands precludes in the present case a definite assignment of bands to such transitions.

The excitation spectra of the higher-lying Rydberg states investigated here resemble closely the excitation spectrum of the lowest excited singlet state in terms of vibrational frequencies as well as transition intensities. The dominant features in the excitation spectrum of each of these states are associated with the "cage squashing" mode ν_{14}, in agreement with what would be expected for excitation of an electron from the lone-

TABLE 3: Experimental Vibrational Frequencies (cm^{-1}) and Intensities of $(\nu_i)_0^1$ Transitions in the Fluorescence-Detected Excitation Spectra of Excited Singlet States of AADA

		$S_2(1\ ^1E)^a$		$S_3(3\ ^1A_1)^a$		$S_1(2\ ^1A_1)^b$		$D_0(1\ ^2A_1)^c$	
mode		freq	int[d]	freq	int[d,e]	freq	int[d]	freq	int[d]
a_1	ν_{15}	451	45	450	50	457.3	36	460.2	30
	ν_{14}	615	126	616	175	618.8	124	623.3	113
	ν_{13}	757	35	756	50	756.3	18	759.6	32
	ν_{12}	782	8			773.6	4	791.7	10
	ν_{11}	888	61	884	50	887.0	22	891.5	55
	ν_{10}	1009	64	1007	200	1005.9	90	1021.1	46
	ν_9	1073	30			1090.3	16	1096.2	6
	ν_8					1244.2	12	1286.1	64
	ν_7					1322.5	23	1365.8	6
	ν_6					1487.4[f]	5	1516.7	1
	ν_5							1549.5	3

[a] Present work. [b] Results obtained in fluorescence excitation studies of the $S_1 \leftarrow S_0$ transition.[7] [c] Frequencies and intensities predicted from (U)B3LYP/6-311G* calculations on equilibrium geometry and harmonic force field of the ground state of the neutral molecule and its radical cation.[7] [d] Intensities taken with respect to intensity of 0_0^0 transition, which is taken as 100. [e] On account of the low intensities of these transitions with respect to the transitions to S_2, partial overlap with hot band transitions, and a rising baseline, these intensities should be considered more qualitative than quantitative (see text). [f] The 6_0^1 transition to S_1 could previously not be identified unambiguously.

TABLE 4: Selected Geometrical Parameters (Å, deg) of the Equilibrium Geometry of the Ground State of AADA (S_0) and Its Radical Cation (D_0) and of the First (S_1) and Second (S_2) Excited Singlet States

	$S_0(1\ ^1A_1)^a$	$S_1(2\ ^1A_1)^{b,e}$	$S_2(1\ ^1E)^{c,e}$	$D_0(1\ ^2A_1)^{d,e}$
$N-C_1$	1.473	−0.012	−0.024	−0.024
C_1-C_2	1.544	0.010	0.019	0.037
C_2-C_3	1.543	−0.002	0.002	−0.005
C_1-H_1	1.096	0.002	0.001	−0.006
C_2-H_2	1.097	−0.001	0.002	−0.004
C_3-H_3	1.097	0.000	0.000	−0.003
$C_1NC_{1'}$	109.6	4.9[f]	5.3	5.5
NC_1H_1	108.3	0.4	0.5	1.6
NC_1C_2	111.7	−7.0	−7.0	−7.1
$C_1C_2H_2$	109.8	−2.3	2.7	−2.8
$C_1C_2C_3$	108.6	0.0	−0.3	−0.7
$C_2C_3H_3$	110.4	−1.0	−0.5	−0.9
$C_2C_3C_{2'}$	109.0	−0.7[f]	−0.4	0.7

[a] B3LYP/6-311G* optimized geometry.[7] [b] Previously reconstructed geometry from $S_1 \leftarrow S_0$ fluorescence excitation studies.[7] [c] Present work. [d] UB3LYP/6-311G* optimized geometry.[7] [e] Given as changes with respect to the geometry of S_0. [f] In a previous publication,[7] these numbers were erroneously given as 6.0 and 0.4, respectively.

pair orbital to a nonbonding Rydberg orbital. When the activity of the other modes is considered, a similar agreement is observed. Qualitatively, it can therefore be concluded that the geometries of the molecule in these three excited states are very similar and, with respect to the totally symmetric vibrations, their force fields as well. For ABCO we have seen at a more detailed level that the differences in transition intensities in the excitation spectra of S_1 and S_2—in particular the activity of the dominating "cage squashing" mode ν_{12}—indicated a slightly different geometry of the molecule in these two states. A reconstruction of the equilibrium geometry of S_2 leading to the geometrical parameters reported in Table 4 shows that also for AADA only minor changes are necessary to account for the observed transition intensity differences. Moreover, it is observed that, compared to the first excited singlet state, the equilibrium geometry of the second excited singlet state resembles even more that of its ionic core.

The line width of the 0_0^0 transition to the lowest excited singlet state of AADA was previously found to be similar to that of ABCO.[7] We accordingly expect and find that the decay time of the emission from the vibrationless level of the lowest excited singlet state of AADA (390 ns) is quite long, like that of ABCO (260 ns). The higher excited states of the two compounds do not show such a close similarity in dynamic behavior. Inasfar as the origin of emission is concerned, dispersed emission spectra show that it occurs once again from highly excited vibrational levels of the lowest excited singlet state. For AADA we find, however, that the 0_0^0 transitions to S_2 and S_3 have a natural line width of 3 cm^{-1} and that the emission resulting from excitation of the vibrationless levels of S_2 and S_3 decays with a significantly longer time constant (250 ns). Apparently, both internal conversion from S_2 (S_3) to S_1 and the subsequent decay of highly excited vibrational levels of the latter state occur at lower rates in AADA than in ABCO.

Conclusions

Fluorescence excitation and emission spectra of the 3p Rydberg manifold of the caged amines ABCO and AADA have been obtained under isolated conditions. Excitation spectra have enabled us to determine accurately the core splitting between the $3p_{x,y}$ and $3p_z$ states (641 and 518 cm^{-1} for ABCO and AADA, respectively), which for both compounds have been assigned as S_2 and S_3. Although the electronic structure of both compounds in the excited states is expected to be similar, it was observed that the ratio of the oscillator strengths of the two transitions differs by about a factor of 5 for the two molecules. The vibrational development in the excitation spectrum of S_2 and S_3 has been shown to mimic closely that observed for excitation of the lowest excited singlet state, minor deviations being accountable for by slight differences in the equilibrium geometry of the molecules in the various excited states. In all cases it could be concluded that the geometrical and vibrational properties of the excited states resemble to a large extent those of their ionic core. Emission spectra and measurements of fluorescence decays have demonstrated that the emission that is observed after excitation of S_2 and S_3 should actually be attributed to emission of highly excited vibrational levels of the lowest excited singlet state, implying that excitation of these higher-lying Rydberg states is followed by internal conversion on a picosecond time scale to the lowest excited singlet state.

Acknowledgment. We wish to thank P. G. Wiering for synthesis of 1-azaadamantane, Ing. D. Bebelaar for valuable experimental assistence, and Prof. C. A. de Lange for use of equipment. This research was supported (in part) by the Council for Chemical Sciences of The Netherlands Organization for Scientific Research (CW-NWO).

References and Notes

(1) Dekkers, A. W. J. D.; Verhoeven, J. W.; Speckamp, W. N. *Tetrahedron* **1973**, *29*, 1691.
(2) Worell, C.; Verhoeven, J. W.; Speckamp, W. N. *Tetrahedron* **1974**, *30*, 3525.
(3) Wiering, P. G.; Verhoeven, J. W. *Recl. Trav. Chim. Pays-Bas* **1996**, *115*, 303.
(4) Eckhardt, W.; Grob, C. A.; Treffert, W. D. *Helv. Chim. Acta* **1972**, *55*, 2432.
(5) Eckhardt, W.; Grob, C. A.; Treffert, W. D. *Tetrahedron Lett.* **1973**, *37*, 3627.
(6) Robin, M. B. Higher Excited States of Polyatomic Molecules; Academic Press: New York, 1974; Vol. 1.
(7) Zwier, J. M.; Wiering, P. G.; Brouwer, A. M.; Bebelaar, D.; Buma, W. J. *J. Am. Chem. Soc.* **1997**, *47*, 11523.

(8) Weber, A. M.; Acharya, A.; Parker, D. H. *J. Phys. Chem.* **1984**, *88*, 6087.
(9) Halpern, A. M. *Mol. Photochem.* **1973**, *5*, 517.
(10) Halpern, A. M.; Ravinet, P.; Sternfels, R. J. *J. Am. Chem. Soc.* **1977**, *99*, 169.
(11) Becker, D. P.; Flynn, D. L. *Synthesis* **1992**, 1080.
(12) Halpern, A. M.; Roebber, J. L.; Weiss, K. *J. Chem. Phys.* **1968**, *49*, 1348.
(13) Parker, D. H.; Avouris, P. *Chem. Phys. Lett.* **1978**, *53*, 515.
(14) Kuno, H.; Kasatani, K.; Kawasaki, M.; Sata, H. *Bull. Chem. Soc. Jpn.* **1982**, *55*, 3097.
(15) Avouris, P.; Rossi, A. R. *J. Phys. Chem.* **1981**, *85*, 2340.
(16) Galasso, V. *Chem. Phys.* **1997**, *215*, 183.
(17) Gonohe, N.; Yatsuda, N.; Mikami, N.; Ito, M. *Bull. Chem. Soc. Jpn.* **1982**, *55*, 2796.
(18) Fujii, M.; Mikami, N.; Ito, M. *Chem. Phys.* **1985**, *99*, 193.